NeuroImage 209 (2020) 116433

Contents lists available at ScienceDirect

NeuroImage

journal homepage: www.elsevier.com/locate/neuroimage

Agito ergo sum: Correlates of spatio-temporal motion characteristics during fMRI

Thomas A.W. Bolton [a,b,*], Valeria Kebets [b,c], Enrico Glerean [d], Daniela Zöller [a,b,e], Jingwei Li [c], B.T. Thomas Yeo [c], César Caballero-Gaudes [f], Dimitri Van De Ville [a,b]

[a] Institute of Bioengineering, École Polytechnique Fédérale de Lausanne (EPFL), Lausanne, Switzerland
[b] Department of Radiology and Medical Informatics, University of Geneva (UNIGE), Geneva, Switzerland
[c] Department of Electrical and Computer Engineering, Clinical Imaging Research Centre, Centre for Sleep and Cognition, N.1 Institute for Health and Memory Networks Program, National University of Singapore, Singapore
[d] Department of Neuroscience and Biomedical Engineering, Aalto University, Helsinki, Finland
[e] Developmental Imaging and Psychopathology Laboratory, Office Médico-Pédagogique, Department of Psychiatry, University of Geneva (UNIGE), Geneva, Switzerland
[f] Basque Center on Cognition, Brain and Language, San Sebastian, Spain

ARTICLE INFO

Keywords:
Behaviour
Motion artefacts
Partial least squares analysis
Resting-state fMRI
Spatio-temporal motion

ABSTRACT

The impact of in-scanner motion on functional magnetic resonance imaging (fMRI) data has a notorious reputation in the neuroimaging community. State-of-the-art guidelines advise to scrub out excessively corrupted frames as assessed by a composite framewise displacement (FD) score, to regress out models of nuisance variables, and to include average FD as a covariate in group-level analyses.

Here, we studied individual motion time courses at time points typically retained in fMRI analyses. We observed that even in this set of putatively clean time points, motion exhibited a very clear spatio-temporal structure, so that we could distinguish subjects into separate groups of movers with varying characteristics.

Then, we showed that this spatio-temporal motion cartography tightly relates to a broad array of anthropometric and cognitive factors. Convergent results were obtained from two different analytical perspectives: univariate assessment of behavioural differences across mover subgroups unraveled defining markers, while subsequent multivariate analysis broadened the range of involved factors and clarified that multiple motion/behaviour modes of covariance overlap in the data.

Our results demonstrate that even the smaller episodes of motion typically retained in fMRI analyses carry structured, behaviourally relevant information. They call for further examinations of possible biases in current regression-based motion correction strategies.

1. Introduction

Resting-state functional magnetic resonance imaging (RS fMRI) has been a vibrant and flourishing research topic. Since its advent (Biswal et al., 1995), the assessment of statistical interdependence between brain regions, or functional connectivity (FC), has enabled the determination of large-scale functional brain networks (Damoiseaux et al., 2006; Power et al., 2011; Yeo et al., 2011), and the harvesting of their spatio-temporal properties towards a refined understanding of a constellation of brain disorders (Fox and Greicius, 2010).

One of the most remarkable features of RS fMRI is that such analyses are already feasible from a few minutes of acquisition (Van Dijk et al., 2009). However, the reliance on low amounts of data also requires that the acquired time courses be impeccably cleaned from potential confounding signals. This is even more of a concern as the field starts moving towards time-varying and -resolved analyses, such as dynamic FC (Laumann et al., 2016)—see Preti et al. (2017) for a review—or real-time neurofeedback (Watanabe et al., 2017).

Amongst confounding signal sources, in-scanner head motion of volunteering participants has been a leading cause of investigation. Its deleterious impacts may take many forms, and remain incompletely understood—see Power et al. (2015); Caballero-Gaudes and Reynolds (2017) for reviews. Some years ago, it was discovered that even short-lived episodes of motion might greatly bias FC analyses (Power et al., 2012; Van Dijk et al., 2012; Satterthwaite et al., 2012), and lead to erroneous interpretations in clinical or developmental studies (Deen and

* Corresponding author. Institute of Bioengineering, École Polytechnique Fédérale de Lausanne (EPFL), Lausanne, Switzerland.
E-mail address: thomas.bolton@epfl.ch (T.A.W. Bolton).

https://doi.org/10.1016/j.neuroimage.2019.116433
Received 10 June 2019; Received in revised form 11 November 2019; Accepted 2 December 2019
Available online 11 December 2019

Pelphrey, 2012; Makowski et al., 2019). These observations of motion-biased results further fueled the development of robust post-processing strategies to free fMRI time courses from confounding motion effects.

Thanks to many rigorous and extensive studies (Satterthwaite et al., 2013; Yan et al., 2013; Power et al., 2014; Burgess et al., 2016; Ciric et al., 2017; Parkes et al., 2018), the field has reached a consensus as to what general steps are essential for a viable RS fMRI denoising pipeline. Their specificities, however, remain debated. In short, following the linear realignment of functional images, estimates of motion over time are obtained along three translational directions (left/right, anterior/posterior and dorsal/ventral, respectively termed X, Y and Z in what follows) and three rotational planes (roll, pitch and yaw, respectively referred to hereafter as α, β and γ). Framewise displacement (FD) is then computed as an aggregated measure across these 6 motion parameters,[1] in order to tag data points corrupted by excessive instantaneous motion and exclude them from subsequent analyses.

Estimated motion time courses are then linearly regressed out from the remaining fMRI data,[2] in a matrix of regressors that can be extended to include their quadratic expansions, their derivatives, and/or their squared derivatives. More parsimonious models lead to a greater amount of retained degrees of freedom in the data, while more exhaustive models may remove signal of interest (Bright and Murphy, 2015), but enable to account for biophysically relevant nonlinear motion effects (Friston et al., 1996).

Finally, the addition of a covariate for group-level analyses has also been warranted (Ciric et al., 2018). However, this last step has been criticised for its risk of biasing some RS fMRI analyses: indeed, if the behavioural feature of interest in the study positively correlates with the extent of head motion, the investigated metric will be more strongly attenuated in larger movers, thus potentially lowering the true magnitude of the effect of interest.

To date, such concerns have been raised in attention or impulsivity studies (Kong et al., 2014; Wylie et al., 2014). Head motion has been posited to be a marker of cognitive control abilities (Zeng et al., 2014), showing clear heritability (Couvy-Duchesne et al., 2014), even if solely non-scrubbed frames are considered (Engelhardt et al., 2017), and sharing genetic influences with hyperactivity (Couvy-Duchesne et al., 2016) or body mass index (Hodgson et al., 2016). Very recently, an extended multivariate assessment isolated body mass index and weight as the major predictors of head motion, with mild additional impacts of impulsivity levels and alcohol/nicotine consumption (Ekhtiari et al., 2019). Thus, in light of current knowledge, the span of behavioural or clinical measures subject to bias remains limited.

A major shortcoming of all the above studies, however, is the use of average FD over time to quantify head motion levels. In other words, it is implicitly assumed that motion properties remain similar along the course of a scanning session, and do not differ across translational directions or rotational planes—an assumption that does actually not square well with the information available to date; see Wilke (2014). It is likely that the true spatio-temporal complexity of motion is so far overlooked, and that its relationship to behaviour is thus only poorly understood. Since even the most sophisticated motion correction approaches summarised above are still unable to fully remove deleterious motion influences (Yan et al., 2013; Siegel et al., 2016), filling such possible gaps of knowledge is a critical task.

Our first question in the present work was thus whether we could find, consistently across subjects, spatio-temporal head motion properties going beyond time- and space-invariance. Our second question was then whether these more subtle motion profiles would be associated to specific anthropometric features, cognitive properties or personal character traits.

2. Materials and methods

2.1. Motion data acquisition and preprocessing

We considered a set of 951 healthy subjects from the Human Connectome Project—HCP (Smith et al., 2013), scanned at rest (eyes open) over four separate 15-minute sessions at a TR of 0.72 s. For each session, motion was estimated using rigid-body transformation with three translation parameters (along the X, Y and Z axes) and three rotation angles (in the α, β and γ planes respectively highlighting roll, pitch and yaw) with respect to a single-band reference image acquired at the start of each session, and FSL's FLIRT (Jenkinson et al., 2012). It resulted in 6 time courses (one per motion parameter) with 1200 time points each.

In the present work, we solely analysed the motion time courses (not the fMRI data) from the first and second acquired sessions (in the main results and to assess replicability of the findings, respectively). Individual motion time courses were differentiated so that our analyses would focus on instantaneous displacement from time t to time t+1. Further, since time points linked to excessive displacement are typically removed from RS fMRI analyses, we only considered non-scrubbed motion instances according to Power's FD definition (Power et al., 2012) at a threshold of 0.3 mm. Resorting to a more conservative (0.2 mm) or more lenient (up to 1 mm) threshold, or censoring not only tagged time points (time t) but also the following ones (time t+1), did not modify our findings (see Supplementary Material, Section 2 for a more detailed description).

2.2. Spatio-temporal motion characterisation

We wished to assess whether different subjects would present distinct spatio-temporal motion characteristics in the data points that are typically conserved in RS fMRI analysis (*i.e.*, not scrubbed out).

For each motion time course, we computed absolute valued instantaneous displacement. Thus, we did not consider the sign of the changes (*e.g.*, moving positively as opposed to negatively in the X direction); this is because initial analyses indicated that positive-valued and negative-valued movements always compensated, to the exception of the X case (two-sided Wilcoxon rank sum test, $p < 0.0001$).

Then, we averaged motion values within each motion type (X, Y, Z, α, β and γ), and each of 6 even-duration time intervals along the scanning sessions (2.4 min = 144 s each). This resulted in a total of 36 conditions. We chose 6 temporal sub-bins to give equal weight to spatial and temporal domain information in our decomposition of the data. Eventually, the values were z-scored across subjects for each condition so that positive values highlight strong movers (at a given time and for a given motion parameter) with respect to the mean, and *vice versa*. It also follows that an equal weight is given to each condition.

Next, we used these 36 motion summary measures to separate subjects into different subgroups of movers through spectral clustering (Von Luxburg, 2007), a nonlinear dimensionality reduction approach—see Supplementary Material, Section 3 for details. By taking into account such precise motion characteristics, we exploit complex motion profiles rather than simply dividing into high- and low-motion subjects, as is classically done on the basis of average FD.

To evaluate whether there was any significant effect of scanning duration, motion parameter or mover subtype, or any interaction between these factors, we conducted a three-way ANOVA (factor 1: scanning duration [time], factor 2: motion parameter [space], factor 3: mover subtype [group]) and assessed significance by comparing the obtained F-values with a null distribution generated non-parametrically over 10,000 folds, shuffling the three factors independently from each other across

[1] Here, we will be discussing the FD metric suggested by Power et al. (2012), but other alternatives have also been put forward in the past literature (Jenkinson et al., 2002; Van Dijk et al., 2012).

[2] Scrubbed data points can be accounted for in two ways: either by modelling them as individual single-point regressors (Lemieux et al., 2007), or by extracting fitting weights from solely non-scrubbed data points, and then applying the regression to the whole data (Power et al., 2014).

subjects.

To assess motion changes along time within a given group of subjects, a linear model was fitted along the six time bins (including a constant regressor of no interest), and the null hypothesis that the mean value across subjects would be equal to 0 was assessed. To examine differences in motion along space, we conducted pair-wise two-tailed t-tests between all group pairs.

2.3. Replication of the findings on a second HCP session

To assess the generalisability of our findings, we performed a similar analysis on a second session from the HCP, acquired during the same day as the first. We matched the 36-dimensional motion states obtained from both sessions using the Hungarian algorithm (Kuhn, 1955), and computed the mean square error (MSE) between the matching pairs. We compared the resulting values to the distribution of MSE values obtained by comparing all possible non-matched pairs of states within or across both sessions.

In addition, to provide quantitative evidence that mover subgroups are the reflection of individual traits, we conducted supervised classification: the mover subgroup of a subject was determined from spectral clustering on one of the two sessions' data, and we then assessed whether that subject would be classified as expressing the same motion state using data from the other session.

For this analysis, we discarded the subjects that expressed, in one of the two sessions, a state that had no equivalent in the other. On the remaining pool of subjects, we quantified the fraction of "correct classification" (*i.e.*, to the same mover subgroup). We conducted the analysis using a K-nearest neighbour classifier with 50 or 100 neighbours, and using either the first or the second session data to generate labels.

2.4. Behavioural data acquisition and processing

For each subject, a battery of behavioural scores was also quantified. A list of all the investigated scores in the present study can be found in the Supplementary Material (Section 4). They were subdivided into several key sub-domains, largely following the original classification found in the *HCP Data Dictionary*[3]:

- Bodily features, such as weight, height or blood pressure.
- Arousal, assessed in terms of cognitive status—MMSE (Folstein et al., 1983)—and sleep quality—PSQI (Buysse et al., 1989).
- Cognitive functions, quantified by diverse scores including, for instance, attentional and memory performance, language skills, and spatial orientation abilities.
- Affect in terms of emotion recognition, anger, fear, stress or life satisfaction—assessed through the NIH toolbox (Gershon et al., 2010).
- Task performance (in terms of accuracy, response time or errors) across various cognitive domains—see Barch et al. (2013) for details.
- Motor abilities, including endurance, gait speed, dexterity and strength measurements.
- Personality, as assessed by the NEOFAC questionnaire (McCrae and Costa Jr, 2004).
- Sensory perception, quantified in terms of responses to noise, odour, pain, taste, or contrast.
- Personal character traits, including for example measures of anxiety, aggressiveness, withdrawal or inattention (Achenbach, 2009).
- Substance use, that is, intake of alcohol or drugs (partly from the SSAGA questionnaire).

For some scores, several entries were not acquired in a sub-fraction of subjects. This was taken into account in behavioural data processing so that it would exert a minimal effect on the described findings. Some scores were also discarded due to various criteria, and the remaining ones were processed as in Smith et al. (2015), yielding a total of 60 summarising measures for subsequent analyses, reflective of anthropometric properties, cognitive abilities or personal character traits. Details are provided in the Supplementary Material (Section 4).

[3] Ωhttps://wiki.humanconnectome.org/display/PublicData/HCP+Data+Dictionary+Public-Ω+Updated+for+the+1200+Subject+Release.

2.5. Univariate links between motion subgroups and anthropometry/behaviour

To determine whether some anthropometric/behavioural scores would differ across mover subgroups, we performed a univariate assessment. For each of the 60 assessed domains, we computed a score indicative of cluster-to-cluster distinction. Formally, following Gu et al. (2012):

$$F(\mathbf{x_i}) = \frac{\sum_{k=1}^{K} n_k (\mu_{k,i} - \mu_i)^2}{\sum_{k=1}^{K} n_k (\sigma_{k,i})^2}, \quad (1)$$

where $\mathbf{x_i}$ is the vector of the ith domain scores across subjects, μ_i is its average regardless of group classification, $\mu_{k,i}$ is its average within group k, and $\sigma_{k,i}$ is the standard deviation within group k. A large $F(\mathbf{x_i})$ score value indicates that the assessed behavioural domain shows distinct values between clusters.

To non-parametrically extract significant scores, we used permutation testing, by randomly shuffling subject motion entries 1000 times. P-values were Bonferroni corrected for 60 tests. Scores were considered significant at a corrected p-value of 0.05.

2.6. Multivariate links between motion features and anthropometry/behaviour

To go beyond univariate comparisons and test for multivariate patterns of motion-behaviour interactions, we conducted a Partial Least Squares (PLS) analysis (McIntosh and Lobaugh, 2004; Krishnan et al., 2011). We summarise the gist of the approach below, and additional details can be found in the Supplementary Material (Section 3).

We considered the matrix of behavioural scores (size 951 × 60) on the one hand, and the matrix of spatio-temporal motion features (size 951 × 72) on the other (where we jointly considered the 36 features obtained from each HCP session). Using PLS, we derived a set of so-called *components*. Each consists in a linear combination of motion scores, and a linear combination of behavioural scores, with maximised covariance. The associated weights are termed *motion saliences* and *behavioural saliences*, and are respectively arranged in $\mathbf{U}$ and $\mathbf{V}$, two matrices of size 72 × 60 and 60 × 60. Motion saliences (*i.e.*, the columns of $\mathbf{U}$) are orthonormal, and so are behavioural saliences. Successive components explain gradually less of the covariance present in the data, as quantified by their *singular values*. Finally, the extent to which a motion salience or a behavioural salience is expressed in a given subject is termed the *motion latent weight* or *behavioural latent weight*, respectively.

To assess significance of the PLS components, we compared their singular values to a null distribution constructed from 1000 shuffled datasets (where shuffling was applied across different subjects), following Zöller et al. (2017). We focused our interpretation on the components significant at $p = 0.05$. To determine the stability of the saliences, we performed bootstrapping with 80% of the data.

For interpretation, we converted the 36-element motion saliences obtained from PLS analysis for each session into a 6-element space and a 6-element time representation, by averaging across all time points or across all spatial directions, respectively. Stability was assessed on these summarising values. Each behavioural or motion salience element was considered significant above a bootstrap score (mean salience across bootstrapping folds divided by the associated standard deviation) of 3, corresponding to a confidence interval of approximately 99% (Garrett

et al., 2010; Zöller et al., 2017).

In addition, we performed correlation analyses between motion (or behavioural) latent weights of the analysed components and FD (as computed from non-scrubbed frames) or age, using Spearman's correlation and non-parametric significance assessment. We also performed a Wilcoxon rank sum test to probe for possible differences in motion (or behavioural) latent weights across gender. Results were Bonferroni-corrected for 24 tests (4 components examined in terms of 3 separate parameters for 2 types of latent weights) and judged significant at a corrected p-value of 0.05.

2.7. Validation of the findings on an independent dataset

To demonstrate that our findings generalise to other acquisition settings, we extracted spatio-temporal motion states, and motion/behaviour modes of covariance, in a second independent dataset. We selected the UCLA Consortium for Neuropsychiatric Phenomics dataset—referred to as the "UCLA dataset" in what follows (Poldrack et al., 2016), which includes healthy subjects as well as patients diagnosed with schizophrenia, schizoaffective disorder, bipolar disorder, and attention deficit/hyperactivity disorder. By this mean, on top of validating our main findings, we could also evaluate whether neuropsychiatric disorders modulate in-scanner motion along space and time, as well as its links with behaviour.

To evaluate whether motion and/or behavioural latent weights were expressed differentially as a function of diagnosis, we conducted a three-way ANOVA (factor 1: significant component index, factor 2: type of latent weight, factor 3: diagnosis), and assessed significance by comparing the obtained F-values with a null distribution generated non-parametrically over 10,000 folds, shuffling the three factors independently from each other across subjects.

3. Results

3.1. Spatio-temporal motion diversity

Average motion across six even-duration time bins, and the 6 motion parameters, was quantified. This spatio-temporal motion profile characterisation revealed the existence of four separate subgroups of movers (Fig. 1A/B). As an alternative representation, we also individually plotted scanning duration or motion parameter against cluster assignments (Fig. 1C), averaging over all entries from the other factor (*e.g.*, the bar labeled "X" denotes the average of motion along the X direction from t_1 to t_6).

In the first mover subgroup ($n_1 = 164$, red patches), subjects showed particularly strong motion in the γ rotational plane. In the second ($n_2 = 310$, dark blue patches), they showed low motion across all time and motion dimensions (negative z-score values in Fig. 1C). In the third group ($n_3 = 282$, green patches), subjects showed particularly marked motion along Y, Z and α. Subjects from group 4 ($n_4 = 195$) moved more from the second session sixth, mostly along X, Z and β.

Statistical analysis confirmed the above observations: on top of a significant effect of group ($F = 3280.21$, $p < 10^{-5}$), there was a significant time × group interaction ($F = 3.19$, $p < 10^{-5}$), and *post-hoc* assessment revealed that while groups 1 and 2 and showed a decrease in motion over time ($\beta_1 = -0.0099$ $[-0.0149, -0.0049]$, $p = 1.35{\cdot}10^{-4}$; $\beta_2 = -0.0034$ $[-0.0051, -0.0017]$, $p = 1.27{\cdot}10^{-4}$), group 4 exhibited an increase ($\beta_4 = 0.0241$ $[0.0136, 0.0347]$, $p = 1.06{\cdot}10^{-5}$). Thus, different mover subgroups displayed varying temporal changes in their extent of motion.

In terms of spatial properties, there was a significant effect of space ($F = 19.65$, $p < 10^{-5}$), as well as a significant space × group interaction ($F = 415.88$, $p < 10^{-5}$). Exhaustive results from a *post-hoc* assessment are displayed in the Supplementary Material (Section 1). They show that subjects in group 1 moved the most in the γ plane (hence their blue shade in Fig. 1B, right panel), while subjects in group 2 moved the least across all 6 spatial degrees of freedom. Group 4 featured the largest movers in X and in β, and group 3 in Y and α. Overall, each group could thus be clearly distinguished on the basis of spatial motion properties.

In a second acquired session, three subgroups of movers could be delineated (Fig. 2A). Each could be unequivocally matched to an equivalent spatio-temporal motion state from session 1 (Fig. 2C, top panel); only the first mover subgroup from session 1 (primarily highlighting marked motion along the γ rotational plane) had no equivalent in session 2. Within the subjects that belonged to one of the three consistently retrieved mover subgroups in session 1, 69.3% continued to belong to the same group in session 2 (Fig. 2C, bottom panel). The converse was also true: 69.4% of subjects expressing one of these three states in session 2 also expressed the same in session 1.

3.2. Univariate links between motion and anthropometry

Next, we related the spatio-temporal motion characteristics of the subjects (as summarised by their mover group assignment) to their anthropometric, cognitive and personality features. Weight, height, blood pressure, language abilities and endurance scores were significantly different across mover subtypes following Bonferroni correction (Fig. 3A). When applying FDR correction instead, scores reflective of sleep disturbances, cognitive flexibility, self-regulation, spatial orientation abilities, and working memory performance also became significant.

Subsequent inspection of pair-wise group relationships (Fig. 3B) showed that group 4 (*i.e.*, the largest movers in X and β) showed greater weight, lower height, more elevated blood pressure and reduced endurance compared to all others, highlighting that they clearly stand out in terms of anthropometric features. Subjects from group 2 (the lowest movers) showed significantly better cognitive abilities compared to all others in language proficiency and self-regulation. They also outperformed subjects from groups 3 and 4 (both larger mover subgroups) in terms of working memory performance, spatial orientation abilities, and cognitive flexibility. Groups 1 and 2 differed more subtly, mostly in terms of endurance (lower in group 1) and height (larger in group 2). Overall, mover subgroups can thus be subdivided in terms of a set of anthropometric and cognitive measures.

3.3. Subtler motion/behaviour relationships revealed by multivariate analysis

Finally, we attempted to extract significant multivariate relationships between our spatio-temporal motion characteristics and the entire breadth of anthropomorphic and behavioural features (Fig. 4).

There were four significant covariance components. Component 1 ($p < 10^{-5}$) explained 79.94% of the data covariance. Its expression was linked to quite uniform, significant motion across all spatial degrees of freedom, along all time bins, and across both sessions (Fig. 4A, left column). The subjects expressing this component more positively had a larger weight and a more elevated blood pressure (Fig. 4B, first row). They showed a greater extent of sleep problems, and reduced cognitive performance across a broad range of domains including cognitive flexibility, inhibitory control, language abilities, processing speed, theory of mind and working memory. Emotion recognition was impaired, and negative affect more pronounced. This was also accompanied by worse endurance, a less daring personality, and a more antisocial, inattentive, externalising and aggressive character. When compared to the mover groups derived beforehand, the gradient in motion latent weights across subjects appeared to discriminate low movers (group 2) from the large movers in group 4 (Fig. 4C, top left panel).

Component 2 ($p < 10^{-5}$) explained 7.74% of the covariance of the data. It contrasted translational (X across sessions, Y in session 1, Z in session 2) and rotational (α and β) motion. Stronger rotational and lower translational movers showed smaller weight, height and blood pressure, lower fluid intelligence, as well as worse inhibitory control, spatial orientation and language abilities. They were less strong and had lower

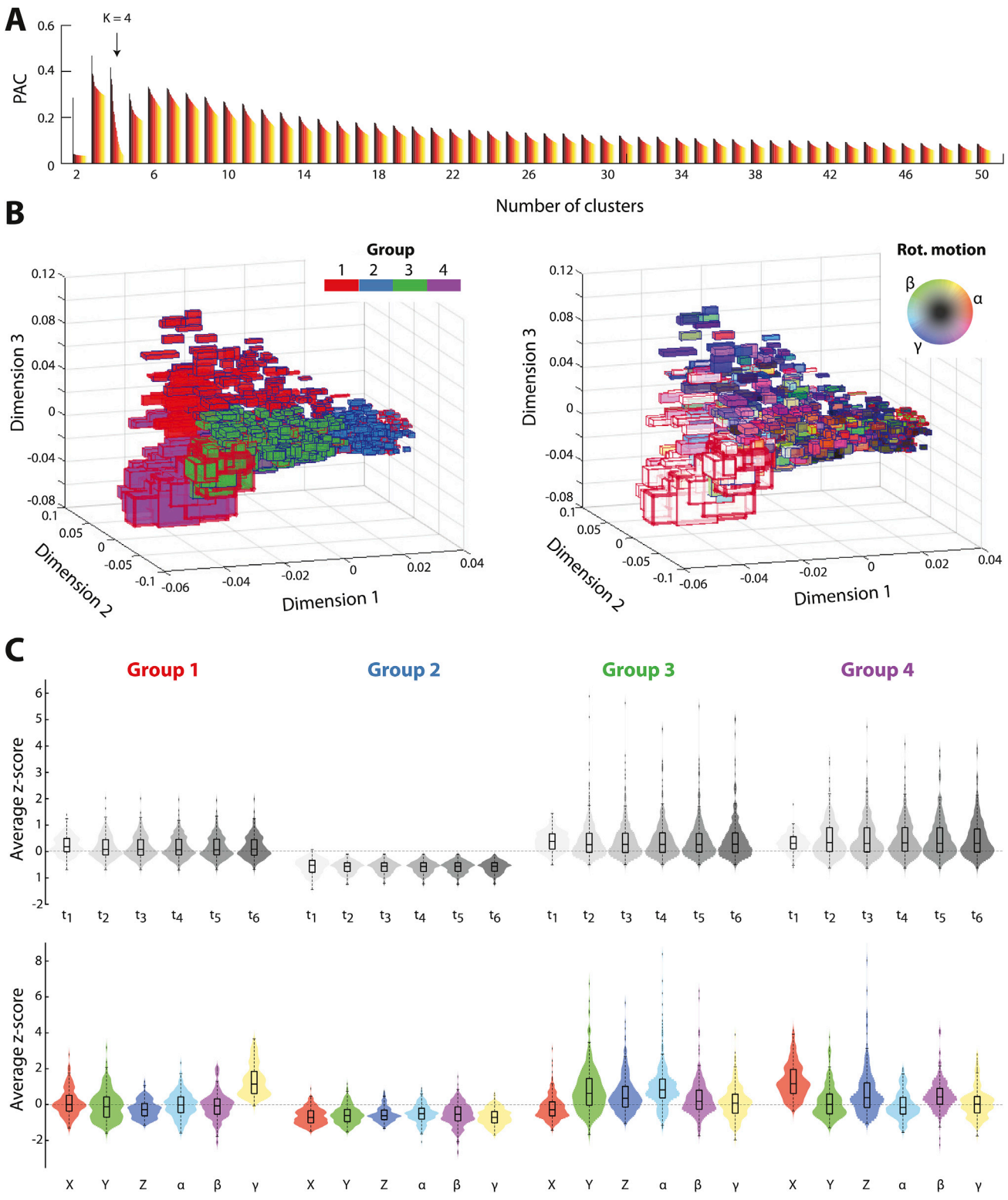

Fig. 1. Groups of spatio-temporal movers. (A) Proportion of ambiguously clustered pairs (PAC) across different evaluated numbers of clusters. The colour gradient from black to yellow denotes PAC evaluation for an increasingly narrow distribution range. Lower values highlight stronger robustness of clustering, and the optimum ($K = 4$) is labeled by an arrow. **(B)** (Left) Dimensionally reduced representation of all 951 subjects, each depicted by a three-dimensional box. Box widths along the first, second and third dimension are proportional to the average motion extent, across all 6 considered time bins, in the X, Y and Z directions. Colours denote the four different subgroups of movers. Edge thickness of the boxes is proportional to the slope of a linear fit to average spatial motion over the 6 temporal bins, while red/blue symbolises increased/decreased motion over time. (Right) Similar representation, with colour coding in RGB scale proportional to the extent of motion in the α (red), β (green) and γ (blue) rotational planes. Black/white denotes uniformly low/high motion along the three rotational planes. **(C)** Simplified representation of the data along time and clusters (top row), or along space and clusters (bottom row).

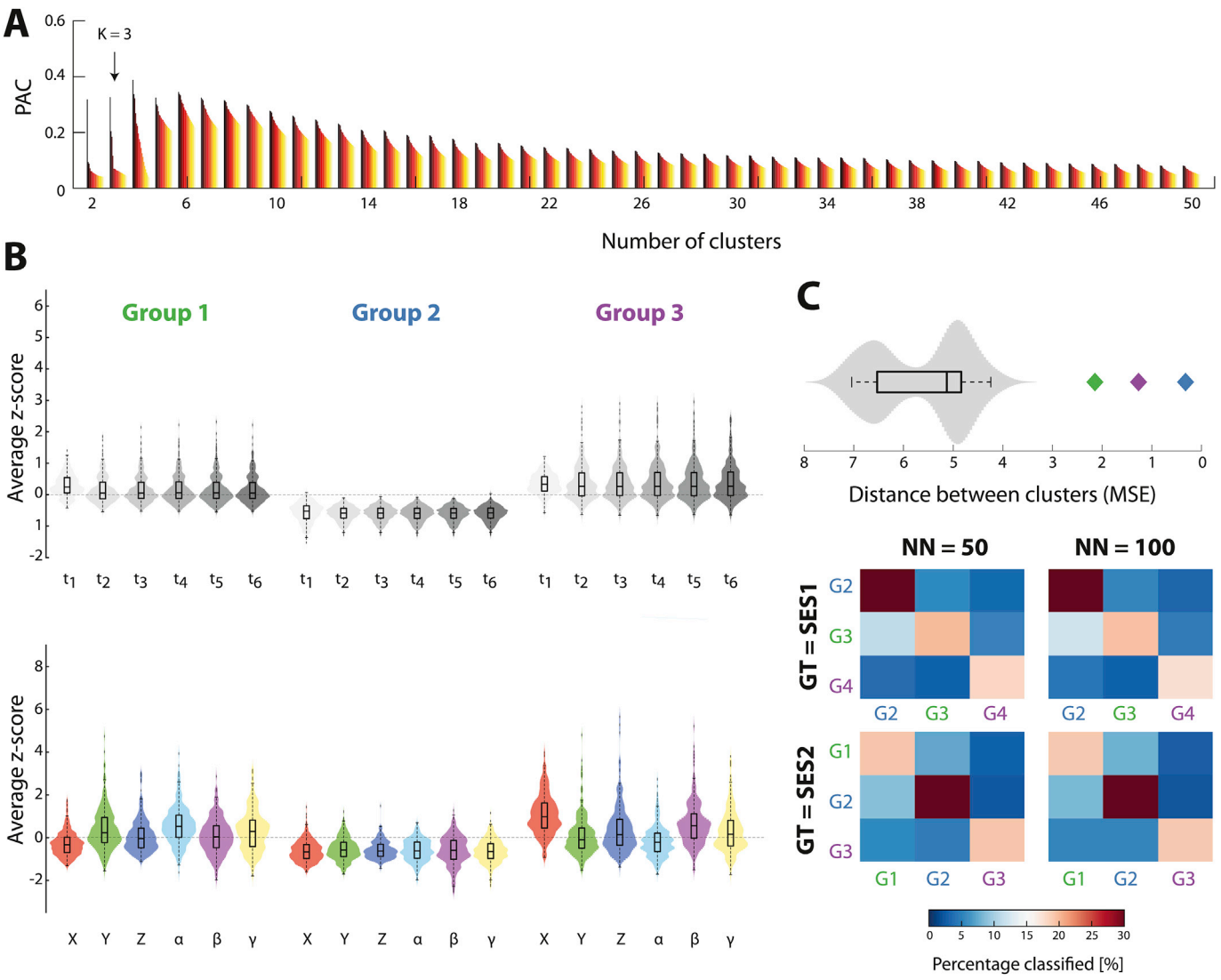

Fig. 2. Replication on a second session. (A) Proportion of ambiguously clustered pairs (PAC) across different evaluated numbers of clusters. The colour gradient from black to yellow denotes PAC evaluation for an increasingly narrow distribution range. Lower values highlight stronger robustness of clustering, and the optimum ($K = 3$; compare with Fig. 1A) is labeled by an arrow. **(B)** Simplified motion representation of session 2 data along time and clusters (top row), or space and clusters (bottom row). Group labels are colour coded according to their matching pattern from session 1. **(C)** (Top) Mean square error (MSE) between matched pairs of spatio-temporal motion states across HCP sessions (coloured data points), and null distribution of MSE values computed between all non-matched pairs of states. (Bottom) When determining the label of a subject (in terms of which motion state it expresses) from session 1 data (top row) or session 2 data (bottom row), percentage of "correctly classified" subjects from motion parameters computed on the other session. Only the subjects that expressed one of the three session 2 states across both sessions are included. Classification was conducted with a *K*-nearest neighbour classifier, using 50 (left column) or 100 (right column) neighbours. GT: ground truth. SES1: first session. SES2: second session. NN: number of nearest neighbours. G1–G4: group 1–group 4.

endurance, but showed greater dexterity. They were also more sensitive to odours and tastes, and overall less prone to negative personal character traits.

Component 3 ($p = 0.006$) explained 4.58% of data covariance, and contrasted translational motion along the X direction with motion along Y, and to a lesser extent, also Z. Lowered motion along X was accompanied by greater height, overall worse cognitive performance (and poorer performance at the mini-mental state examination), and a more negative affect. This was complemented by a greater perception of pain, more pronounced withdrawal habits, thought problems, aggressiveness and hyperresponsiveness. Motion latent weights were most positive for subjects from group 4, and for a subset of subjects from group 3 that showed a similar tendency for increased motion along time (see the red edges of the associated boxes in Fig. 1).

Finally, component 4 ($p = 0.008$) explained 2.2% of the motion/behaviour covariance, and largely corresponded to movement in the γ plane during session 1 (but not session 2, as the associated bootstrap score did then not reach significance). Expectedly, latent motion weights were positive for the subjects belonging to group 1. Behaviourally speaking, a more pronounced expression of this component was not associated to bodily features, but related to greater sleep problems, better cognitive flexibility, a more positive affect (as seen from enhanced psychological well-being and social relationship scores), less conservative and more daring gambling habits, and a more introverted personality. Globally more negative personal character traits, especially including greater anxiety and depression scores, completed the picture.

Motion latent weights of component 1 positively correlated with mean FD—computed on non-scrubbed frames (Fig. 5A; $R = 0.86$, $p < 0.001$), and so did behavioural latent weights ($R = 0.44$, $p < 0.001$). A gender difference was also seen at the level of motion latent weights ($t = -3.7$, $p < 0.001$, denoting lower values in males). For component 2, there was a positive correlation between behavioural latent weights and age (R

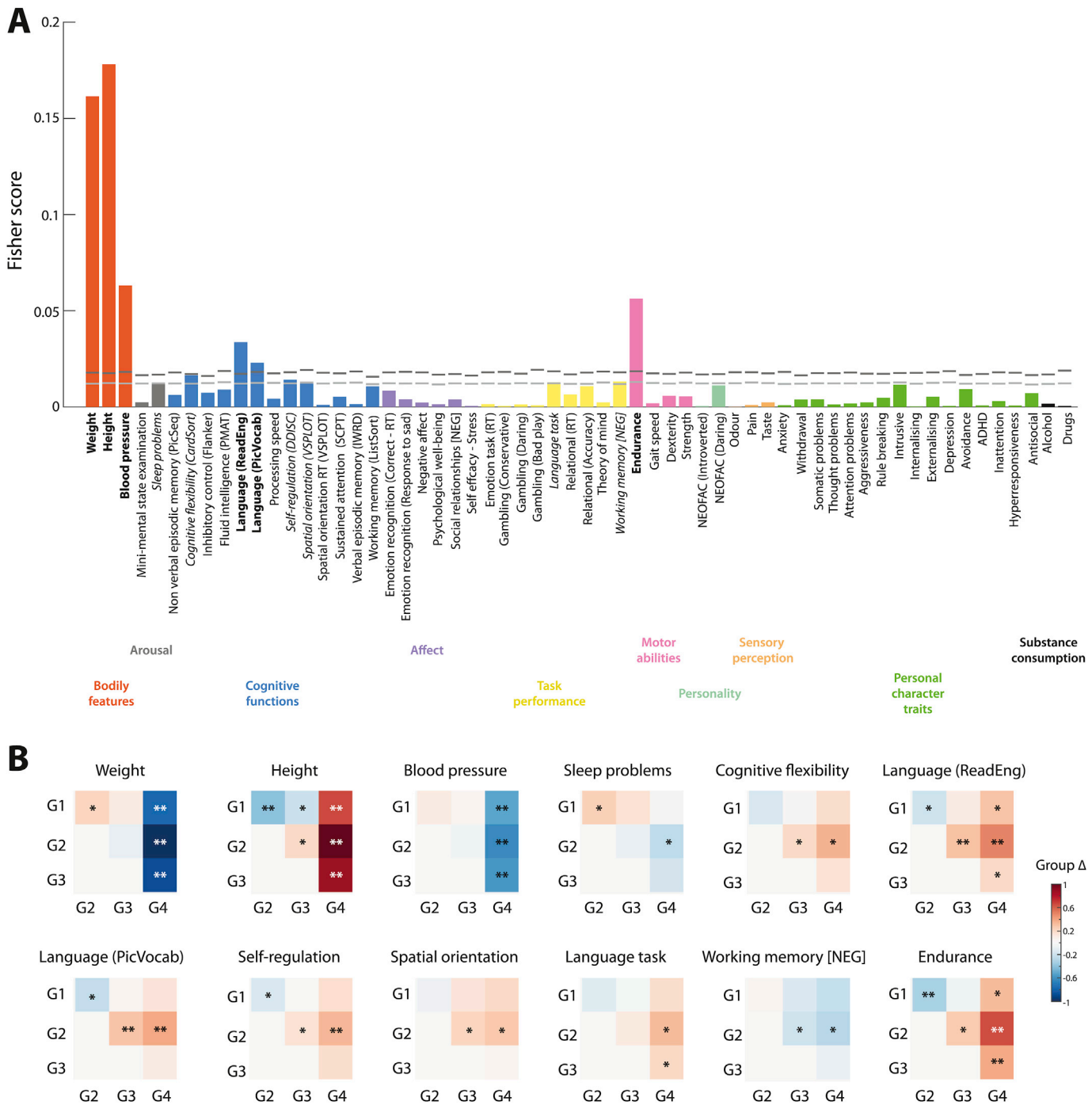

Fig. 3. Univariate links between spatio-temporal motion and anthropometry/cognition/personal character. (A) Across all 60 considered domains, Fisher score in terms of discriminability across the four spatio-temporal mover groups. Black horizontal bars denote significance thresholds, derived non-parametrically and Bonferroni-corrected for 60 tests. Grey bars denote significance thresholds upon FDR correction. The "[NEG]" label for a behavioural score reflects the fact that a more positive value highlights a decrease in the assessed quantity. **(B)** For the 12 significant domain scores, *post-hoc* comparison of Fisher score values across mover subgroups. Positive values highlight stronger scores for the row group. One star (*) highlights significance without multiple testing corrections, and two stars (**) highlight significance upon Bonferroni correction for 72 tests (6 pair-wise comparisons for 12 scores). PicSeq: picture sequence memory. CardSort: dimensional change card sort. PMAT: Penn progressive matrices. ReadEng: oral reading recognition. PicVocab: picture vocabulary. DDISC: delay discounting. VSPLOT: variable short Penn line orientation test. RT: response time. SCPT: short Penn continuous performance test. IWRD: Penn word memory test. ListSort: list sorting. ADHD: attention deficit/hyperactivity disorder. G1–G4: group 1–group 4.

$= 0.21, p < 0.001$), and a strongly significant gender difference seen both from the viewpoint of motion latent weights ($t = -9.04, p < 0.001$) and behavioural latent weights ($t = -23.33, p < 0.001$). Component 3 displayed a significant gender difference for behavioural latent weights ($t = 7.35, p < 0.001$). Finally, for component 4, behavioural latent weights negatively correlated with age ($R = -0.14, p < 0.001$).

3.4. Validation on an independent dataset

The results obtained on the UCLA dataset are presented in Fig. 6. In this case, movers were subdivided into 7 distinct subgroups (see Fig. 6A, where the PAC for $K = 7$ reaches lower values than expected from the global trend). As seen from the low-dimensional summary representation

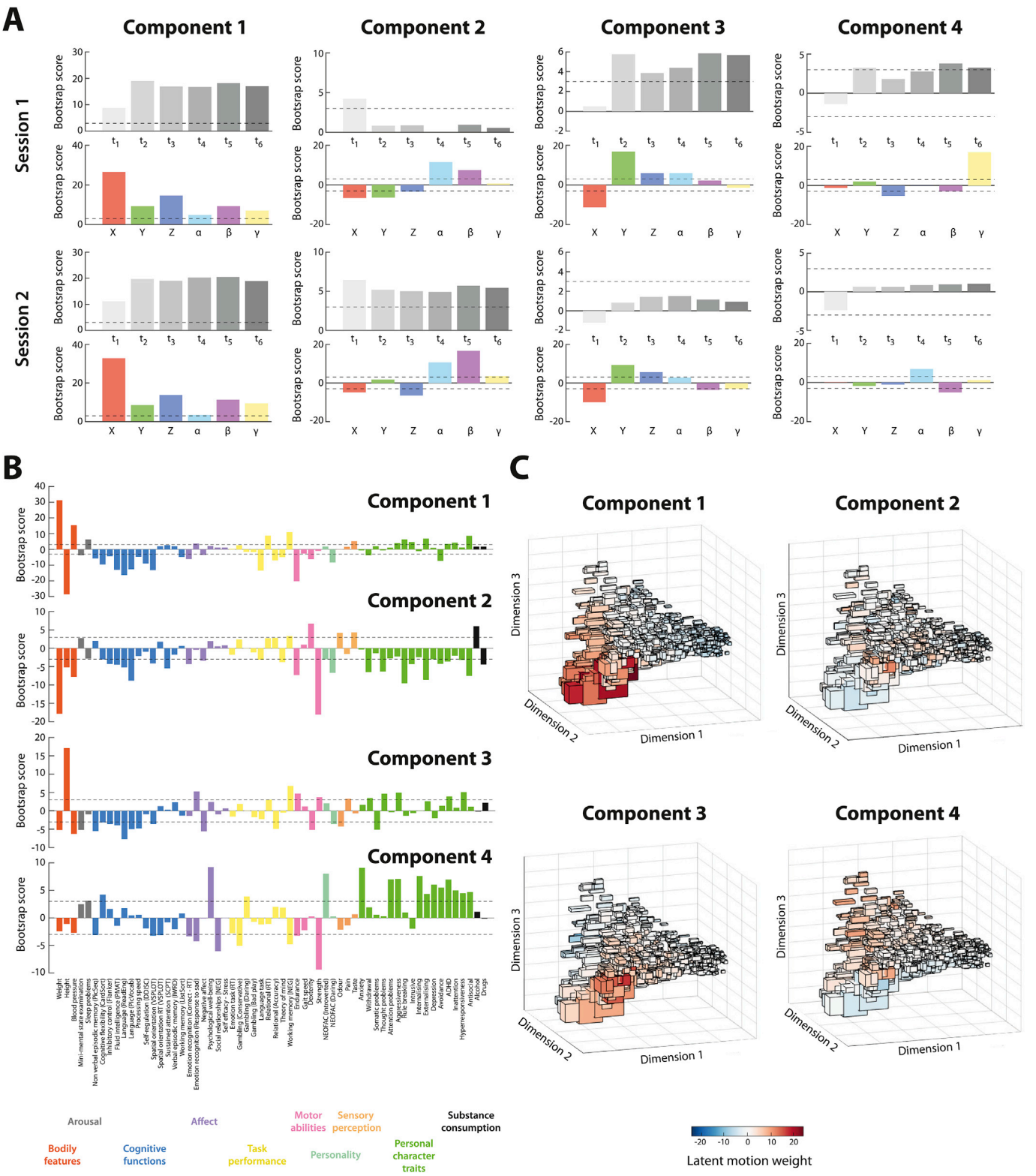

Fig. 4. Motion/behaviour covariance components. (A) For spatio-temporal motion saliences, bootstrap scores in terms of expression over time and spatial motion features, for the first and second HCP sessions (top and bottom pairs of plots). Components 1 to 4 are presented from left to right, and significance thresholds (absolute bootstrap score larger than 3) are denoted by horizontal dashed lines. **(B)** Behavioural saliences for the four components (from top to bottom), with significance thresholds denoted by horizontal dashed lines. The "[NEG]" label for a behavioural score reflects the fact that a more positive value highlights a decrease in the assessed quantity. **(C)** For all four components, representation of motion latent weights in the dimensionally reduced space investigated in clustering analyses (see Fig. 1B). PicSeq: picture sequence memory. CardSort: dimensional change card sort. PMAT: Penn progressive matrices. ReadEng: oral reading recognition. PicVocab: picture vocabulary. DDISC: delay discounting. VSPLOT: variable short Penn line orientation test. RT: response time. SCPT: short Penn continuous performance test. IWRD: Penn word memory test. ListSort: list sorting. ADHD: attention deficit/hyperactivity disorder.

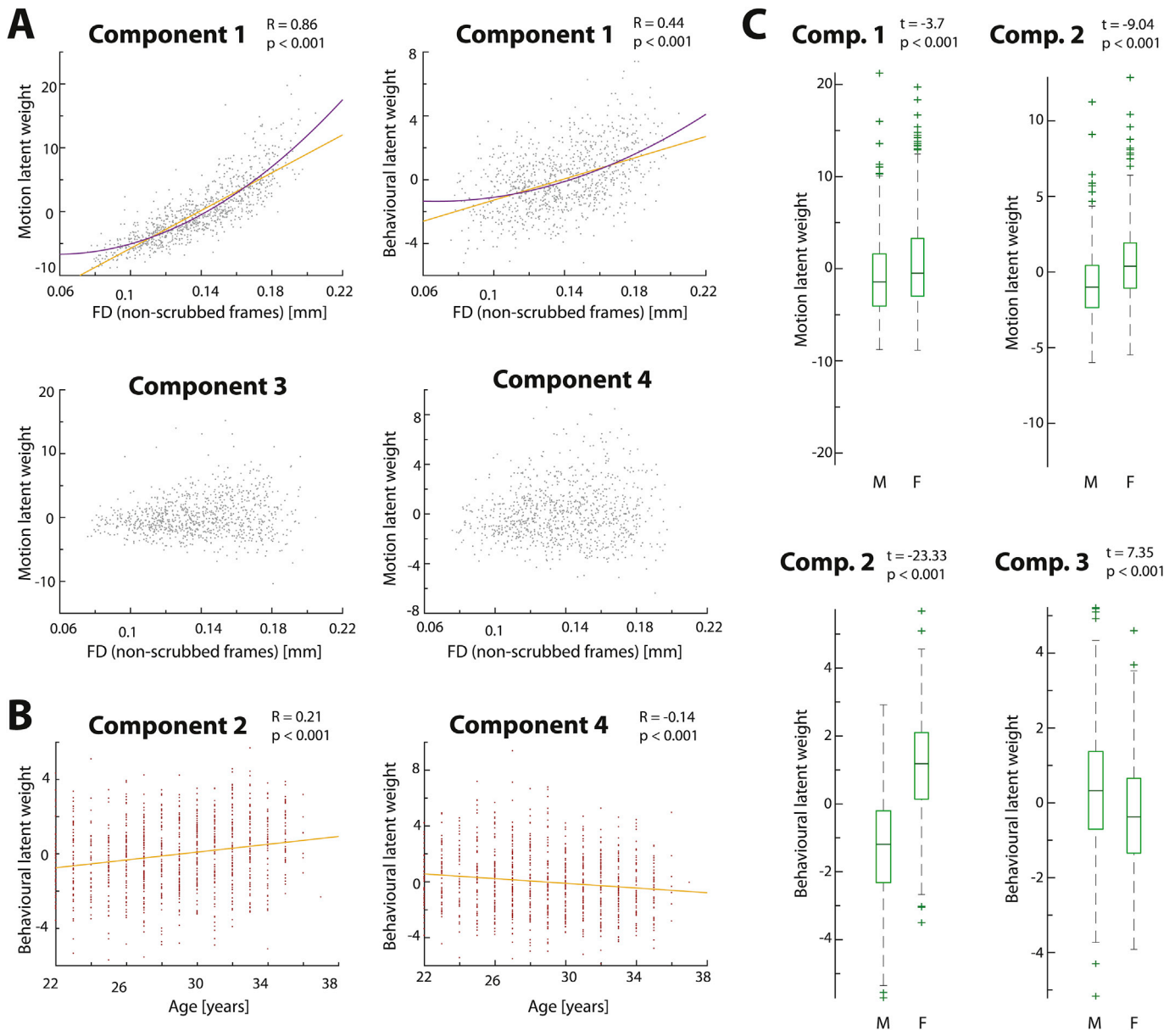

Fig. 5. Relationship of latent weights with mean FD, age and gender. For all four significant components, correlations between behavioural or motion latent weights and mean FD computed on non-scrubbed frames **(A)**, age **(B)** or gender **(C)**. Provided p-values are Bonferroni-corrected for 24 tests. FD: framewise displacement. M: male. F: female.

in Fig. 6A (bottom left panel) and from summary statistics in Fig. 6B, groups 1, 3, 5 and 6 displayed lower motion than the average population along all spatial degrees of freedom, but the exact contribution of given translational and rotational parameters varied across cases. In addition, motion was consistently larger during the second half of scanning. Groups 2, 4 and 7 were associated to larger motion. In groups 2 and 7, it primarily involved the Y and Z directions (more strongly in group 7). In group 4, all 6 parameters were involved. In all three cases, motion tended to decrease from the first to the second half of the acquisition.

Patients diagnosed with attention deficit/hyperactivity disorder (ADHD, red boxes in Fig. 6A, bottom right panel), bipolar disorder (blue boxes), schizophrenia (purple boxes), and shizoaffective disorder (orange boxes) populated all spatio-temporal motion states, and thus largely contributed to the increased diversity seen as compared to HCP analyses.

Three motion/behaviour covariance components reached significance; motion saliences are presented in Fig. 6C, and behavioural saliences in Fig. 6D. Component 1 ($p < 10^{-5}$) explained 89.3% of covariance in the data. Similarly to component 1 in the HCP case, it represented uniform motion along all spatial dimensions and both time bins. A stronger positive expression of this component was associated to larger weight, worse learning and memory performance, impaired task-switching abilities, and lowered continuous performance.

Component 2 ($p = 0.036$) explained 3.52% of the motion/behaviour covariance. It strongly resembled component 3 from the HCP analyses: indeed, it primarily contrasted motion along X and Y, with an expression that reverted in sign from the first to the next time bin. Furthermore, stronger movers along X (and lower movers along Y) also showed a greater delay discounting tendency.

Component 4 ($p = 0.017$) explained 1.71% of the data covariance, and was new. It highlighted larger motion along Z paralleled by lower motion along Y and α. From the behavioural side, the larger Z movers had higher intelligence scores, but also showed worse task-switching abilities.

An ANOVA revealed an effect of the component index on latent

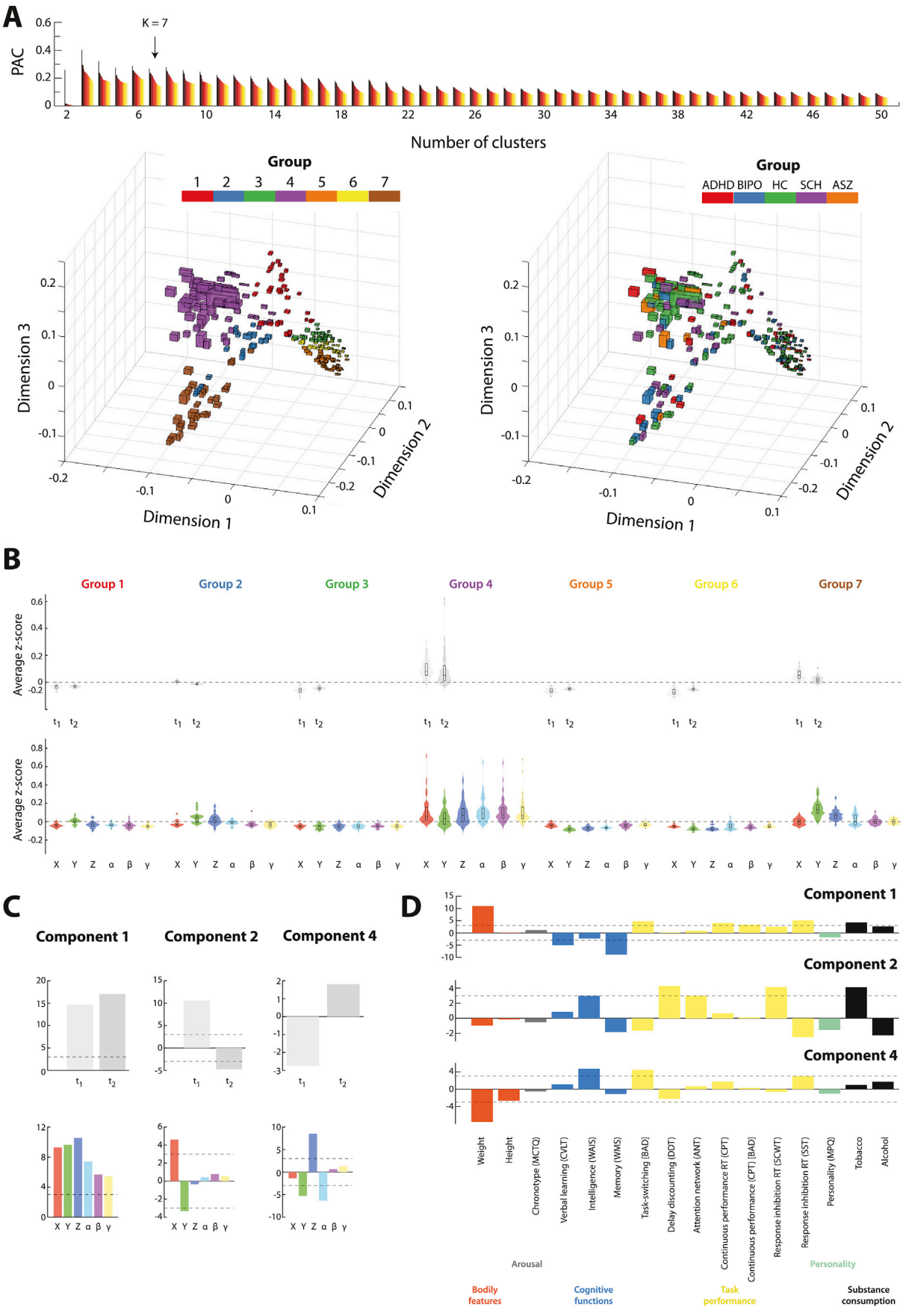

(caption on next page)

Fig. 6. Results on validation dataset. (A) (Top) Proportion of ambiguously clustered pairs (PAC) across different evaluated numbers of clusters. The colour gradient from black to yellow denotes PAC evaluation for an increasingly narrow distribution range. Lower values highlight stronger robustness of clustering, and the optimum ($K = 7$) is labeled by an arrow. (Bottom left) Dimensionally reduced representation of all 245 subjects, each depicted by a three-dimensional box. Box widths along the first, second and third dimension are proportional to the average motion extent, across both considered time bins, in the X, Y and Z directions. Colours denote the seven different subgroups of movers. **(B)** Simplified representation of the data along time and clusters (top row), or along space and clusters (bottom row). **(C)** For spatio-temporal motion saliences, bootstrap scores in terms of expression over time and spatial motion features. Components 1, 2 and 4 are presented from left to right, and significance thresholds (absolute bootstrap score larger than 3) are denoted by horizontal dashed lines. **(D)** Behavioural saliences for the three components (from top to bottom), with significance thresholds denoted by horizontal dashed lines. The "[NEG]" label for a behavioural score reflects the fact that a more positive value highlights a decrease in the assessed quantity. ADHD: attention deficit/hyperactivity disorder. BIPO: bipolar disorder. HC: healthy control. SCH: schizophrenia. ASZ: schizoaffective disorder. MCTQ: Munich chronotype questionnaire. CVLT: California verbal learning test. WAIS: Wechsler adult intelligence scale. WMS: Wechsler memory scale. DDT: delay discounting task. ANT: attention network task. RT: response time. CPT: continuous performance task. SCWT: Stroop colour and word test. SST: stop signal task. MPQ: multidimensional personality questionnaire.

weights ($F = 10.83$, $p < 0.0001$), as well as an effect of diagnosis ($F = 12.34$, $p < 0001$). In addition, there was also a significant component index × diagnosis interaction ($F = 14.99$, $p < 0.0001$), indicating that motion and behavioural latent weights are expressed with different magnitude across components in a way that depends on the diagnosis of the subject at hand. This parallels the findings from another PLS-based investigation of functional connectivity/behaviour covariance, which also highlighted a diagnosis-dependent strength of expression (Kebets et al., 2019).

4. Discussion

4.1. A cartography of in-scanner spatio-temporal motion

In RS fMRI analyses, time points associated with excessive instantaneous motion (as quantified by a composite FD score) are typically removed/scrubbed. Two implied assumptions are made through this process: the first is that motion in the retained, non-scrubbed time points is negligible and does not show any characteristic structure. The second assumption is that FD is sufficient to characterise motion.

Our results question both of the above assumptions. Indeed, we were able to separate scanned volunteers into four different mover subgroups even when excluding time points with high motion as quantified by FD. These groups differed in the extent of motion displayed by subjects along the three translational (X, Y and Z) and three rotational (α, β and γ) motion directions, as well as in the temporal evolution of motion along the scanning session.

More specifically, a change in motion extent along the scanning session was observed, as seen by a significant time × group interaction in our ANOVA design, as well as by significantly non-null *post-hoc* regression coefficients. The absence of time × space, or time × space × group interaction terms means that temporal changes were consistent across all motion directions.

In space, there were strong group differences that contributed in large part to the organisation revealed in the dimensionally reduced representation of Fig. 1B. Two mover subgroups were opposite extremes: group 2 subjects moved very little as compared to the average across spatial directions (hence depicted in black in Fig. 1B, right panel), while the subjects in group 4 consistently displayed very large displacements (hence represented in white), particularly along X, Z and β. Distinguishing features of the last two groups were motion along Y and in the α plane (group 3), or γ motion (group 1, as colour coded by a blue shade).

In addition to spatial motion properties, there were also significant changes over time, and a closer inspection revealed that the main drive of this result was a modified extent of motion after the first sixth of the session (see Fig. 1C): in subjects from group 4, motion increased after the first 2.4 min of recordings, while the opposite was seen for groups 1 and 2.

Our replication analyses on a second HCP resting-state session (Fig. 2) enabled to clarify that these spatio-temporal motion characteristics reflect a mix between subject traits and more punctual, session-specific sources: indeed, mover subgroups 2, 3 and 4 were found back in the second session recordings, and the subjects that belonged to one during a session most often stayed in the same during the other run. This means that these motion configurations are inherent traits of the subjects, who will always show an individualised motion profile.

Subjects from group 1, which highlighted γ motion, only expressed that particular motion state during session 1. This implies that γ motion is not a permanent trait, but rather denotes the adjustment to the scanner environment at the very start of an acquisition (indeed, in HCP recordings, session 1 is acquired immediately after the subject is positioned in the scanner, and session 2 is then acquired consecutively), as further supported by the fact that expression of that motion configuration significantly decreased along the course of session 1. This hypothesis is also corroborated by our validation analyses: γ motion was not detected there, as in UCLA acquisitions, a structural scan precedes the acquisition of the resting-state data.

The need for a few minutes before setting into a motion steady state, and presence of punctual, session-specific motion profiles, raise the possibility of generally unaccounted sources of bias in the data, either across resting-state sessions (if consecutively acquired), or even in structural scans if acquired first upon moving the subject in the scanner. Future work should more exhaustively investigate this possibility by relating individual motion specificities to imaging features *per se*.

All in all, the presence of strongly differing spatial motion profiles across subjects confirms the importance of subject-level motion correction strategies through regression. Further, since our work focused on instantaneous motion (t to $t+1$ changes), our results may be interpreted as an additional argument in favour of more complete regression models, at least to the point of incorporating motion time courses and their shifted counterparts (see below, however, for a more complete discussion).

Rather than considering four subgroups of movers, another perhaps more relevant interpretation of our data is the presence of several axes of motion: the first is a global component, homogeneous across space. It is seen as the first dimension in our spectral clustering investigations (Fig. 1B), positioning it as the major discriminating factor across subjects. It is also found back as the first, most prominent component in the following PLS analysis (Fig. 4A, left column). Other more subtle, but nonetheless significant spatial motion combinations then add up on top: for example, motion along the γ plane is jointly captured in dimensions 2 and 3 in spectral clustering, and component 4 in the PLS analysis.

The two methodological approaches employed strongly differ in their core properties: spectral clustering is a hard clustering technique in which each subject can only be assigned to one group, while PLS describes the motion properties of each subject as a linear combination of motion saliences that co-vary with anthropometry and behaviour. The convergent findings obtained from both analytical perspectives strengthen our newly revealed cartography of spatio-temporal movers as a non-negligible feature. Furthermore, the fact that we also clearly delineate a discrete set of mover subgroups in an independent validation dataset (Fig. 6A/B) is evidence that this spatio-temporal complexity is not specific to fast TR acquisitions, but generalises to other more typical datasets.

Our findings question the accuracy of most motion correction

assessment approaches, which exclusively rely on averaged FD over time. A separate assessment across motion parameters (or more elaborate approaches involving specific weighted combinations, such as our PLS motion saliences) appears necessary to better understand which motion impacts are removed, and which subsist in the data.

4.2. Agito ergo sum: bodily and behavioural underpinnings of motion

In 1644, Rene Descartes, in quest for a primal principle at the root of all knowledge, formulated his notorious "cogito ergo sum" (I think, therefore I am).[4] 375 years later, we wish to summarise our findings by reformulating his words: "agito ergo sum" (I move, hence I am). By this, we mean that the defining aspects of someone (one's bodily features, abilities to interact with the world and ways to respond to the environment around) are reflected, in various and subtle ways, in how one moves during scanning.

As an example of this principle, while subjects from groups 1 and 2 moved less after the first sixth of the recording session, high movers from group 4 moved more. Univariate evaluation following spectral clustering revealed that the latter mostly stood out in terms of anthropometric or fitness measures (Fig. 3B): weight, height, blood pressure and endurance. Conversely, group 2 subjects stood out by their better cognitive abilities.

These observations enable to sketch a global picture of how the response to the scanning environment differs across subjects: low movers, who are able to efficiently cope with changes in environmental conditions and self-regulate themselves (for example, by better adjusting to the loud MRI noise fluctuations), rapidly start moving less and maintain overall low head motion throughout scanning. Large movers, on the other hand, are intrinsically more prone to large head motions, possibly because of feeling more cramped inside the scanner, and become increasingly uneasy with the contiguous MRI environment, thus moving more.

A caveat of univariate approaches is the risk that more subtle behavioural correlates of motion remain undetected. Our follow-up multivariate PLS analysis confirmed this limitation: motion saliences from the most prominent component (Fig. 4A, left panel) were positive across space and time, with an increase following the first session sixth. This means that subjects expressing this component more strongly move more overall, and *vice versa*, as also confirmed by a strong positive correlation with FD (Fig. 5A, top row). This component thus highlights similar motion features as the ones discriminating mover groups 2 and 4. The array of associated behavioural saliences not only included the dominating anthropometric factors mentioned above, but also showed that larger movers have lower fluid intelligence and perform worse in theory of mind or relational tasks. Further, they also exhibit more aggressiveness, inattention and antisocial behaviours.

Overall, this global pattern is highly reminiscent of a positive-negative mode of population covariation previously described by Smith and colleagues (Smith et al., 2015), and put forward as relating behaviour, demographics and FC. The similarity may partly come from the fact that the authors resorted to Canonical Correlation Analysis (CCA), a multivariate technique with strong similarities to PLS. Our results raise the possibility that this mode may, at least in part, reflect differences in motion across the considered subjects.

The main PLS component highlights the dominating factor of motion/behaviour covariance. On top of it, we also revealed subtler overlapping factors. Component 2 contrasted motion along the X/Y/Z translational directions and the α/β rotational planes (*i.e.*, more strongly expressing subjects move more rotationally, but less translationally). Positive motion and behavioural latent weights were seen in females, while the opposite was seen for male subjects (Fig. 5C), implying that gender may be an underlying cause of that particular motion pattern. α reflects roll, occurring in the plane spanned by the X axis: motions along α and X are thus biophysically constrained to occur concurrently. The differential recruitment of both motions across genders may result from distinct anthropometric factors (larger weight, height and blood pressure in males), or from behavioural specificities of one of the genders.

Component 3 primarily contrasted motion between the X and Y translational planes, and like component 1, was retrieved in both the HCP and UCLA datasets. When jointly considering the motion saliences over time and space, one can understand this component as representing a shift, over time, from a configuration where X motion is stronger, to one when motion along Y takes over. Furthermore, this change occurs after the first 2.4 min of scanning, as the temporal salience weights then largely increase from around 0 (HCP session 1), or even revert in sign (HCP session 2 and UCLA). This adjustment of motion over the course of the acquisition arises from a mix between a large set of anthropometric factors, cognitive abilities and personality character traits, as seen from the broad repertoire of significant behavioural salience weights.

Component 4 specifically showcased the γ motion seen in group 1: those subjects that express it strongly move a lot along γ. Note that, in accordance with our results obtained from spectral clustering, γ motion only occurs during session 1, but not session 2 (the bootstrap score does then not reach significance). No significant anthropometric associations were detected, but the subjects expressing component 4 showed stronger sleep disturbances, better cognitive flexibility, as well as a more introverted personality. This was accompanied by a wide scope of elevated personal character trait scores, including anxiety, attention problems, aggressiveness, depression and hyper-responsiveness.

We conjecture that this component may reflect efforts of the subjects to refrain from moving in the scanner: indeed, head motion along γ reflects yaw, and may highlight attempts at limiting translational displacements along X or Z by forcing the head to remain anchored on the bed. The efforts leading to this typical motion signature may be regulated by the subjects' good cognitive abilities, and were perhaps influenced by their personal character traits. This extra care at limiting motion then dissipates progressively along recording time, and is not exerted anymore during subsequent acquisitions.

Interestingly, the expression of components 2 and 4 also correlated with age, despite considering a relatively narrow age range in the present study (between 26 and 35 years old). Since head motion has been a central question in developmental studies, it will be interesting to examine, in future work, whether the characterisation of motion in terms of the translational/rotational balance (component 2), or along γ (component 4), may be a better strategy than through FD (especially given that component 1, accounting for the global motion effect, showed no significant relationship to age).

In addition to the above, we note an interesting dependence between motion latent weights and mean FD in the case of components 3 and 4: as can be seen in the associated plots from Fig. 5A, these weights are expressed with larger magnitude in larger movers, but with a polarity that varies from a subject to the other, as seen by a V-shaped profile in the plots. The interpretation is that in a given subject, there is a baseline level of overall uniform motion along space and time (symbolised by component 1); on top of this, additional trends add up in the case of larger mean FD subjects, and render the motion/behaviour relationships more complex in ways that are space- and time-dependent, and differentially implicate anthropometric and cognitive scores.

4.3. Implications, limitations and future perspectives

Our results have strong implications regarding RS fMRI studies: indeed, the observation that a broad array of behavioural and clinical characteristics relate to motion implies that the scope of studies reporting possibly biased findings with regard to clinical or cognitive group-level comparisons is perhaps much wider than envisaged so far. On top of previously questioned results regarding fluid intelligence (Finn et al., 2015)—see Fig. 6 of Siegel et al. (2016), former reports focusing on

[4] The first mention of that particular formulation indeed dates back from the *Principia philosophiae*, published in 1644.

sustained attention (Rosenberg et al., 2016) or extraversion (Hsu et al., 2018) may also need to be reconsidered.

Earlier on, we discussed how the widely used extended subject-level regression designs enable to remove the spatio-temporally complex motion effects introduced here. However, their intricate and overlapping relationships with behaviour raise the danger that, akin to including average FD as a covariate in group-level analyses, an unwanted bias with regard to clinical or cognitive analyses occurs at the single-subject level stage.

Assume, for example, that an experimenter is interested in studying psychological well-being through assessments of FC at rest. From our results, subjects with a greater positive affect will exhibit a modulated amount of motion along the γ axis, in a way that remains constant from past the first few minutes of an acquisition (Figs. 1C and 4A). The use of a regressor encoding instantaneous motion changes along γ, as suggested by most for optimal data preprocessing, may result in the removal of a larger signal fraction in individuals with more elevated psychological well-being, possibly leading to the underestimation of the effect of interest. For this reason, we encourage experimenters, in future analyses, to investigate the fitting coefficients obtained upon regression so that it can be verified whether a link exists between the extent of removed signal, and the behavioural feature of interest.

Of course, the exact impact of the regression step will depend on the precise temporal expression of γ motion and of positive affect-related fMRI fluctuations, since one fitting coefficient is extracted depending on frame-wise similarities between the considered motion and the voxel-wise fMRI time courses. The obvious next step to perform, and the major limitation of the present analyses, is that we have not yet pushed our exploration to the level of fMRI time courses, but focused on motion estimates only. Our aim, with this report, was not to design a new efficient motion correction strategy, but to dig into the complexity of motion *per se*, and by this mean, put forward possible caveats and improvements of existing approaches. Our code and results are fully available at https://c4science.ch/source/MOT_ANA.git, and we encourage the interested researchers to extend our current investigations at the level of the fMRI signal.

A second limitation of our work is that we solely analysed head motion, although many more factors are known to corrupt the fMRI signal (Bianciardi et al., 2009; Birn, 2012; Liu, 2016). In addition, particularly important for the present analyses is the recent demonstration that an array of physiology-driven components directly contribute to the motion time courses themselves: in the specific case of fast TR acquisitions, as for the HCP data considered here, respiratory artefacts become particularly pronounced, and include mechanical motion of the head due to respiration, as well as quasi-periodic perturbations of the magnetic field resulting in additional *pseudomotion* components in the data (Chen et al., 2019).

Power et al. (2019a) further clarified that at least 5 distinct respiration-related sources of motion are present in fast TR data: first, real motion along Z and β arises at the frequency of the respiratory cycle; second, additional true motion contributions come from short-lived episodes of deep breathes; third, pseudomotion at the respiratory frequency also contaminates the phase-encode direction (in the case of HCP data, the X direction); fourth, deep breathes result in further pseudomotion at a lower frequency around 0.12 Hz; fifth, motion along Y and Z is also modulated by the respiratory envelope. “True”, punctuate head motions, add to these, as well as “bleeding” of respiration-induced oscillations from the main axes that are involved to the others.

At least part of the reported findings here can be expected to relate to such respiratory influences: the fact that weight and height significantly contributed to all but one of the significant PLS components is an indication towards this, as body mass index is strongly tied to respiratory rate as well as pseudomotion effects, due to different biophysical subject properties (Power et al., 2019a). Future analyses shall clarify the exact contribution of respiration to our findings, for instance by resorting to various filtering strategies; however, such approaches are not trivial to implement, as physiological rhythms occur at different frequencies across subjects, and overlaps between pseudomotion-related and true motion-related frequency spans occurs in some, but not all, cases.

It is important to specify that although regression-based approaches are one of the major preprocessing avenues, other motion correction alternatives also exist and may less suffer from possible biases; they include original twists on traditional regression designs (Patriat et al., 2015, 2017), more sophisticated variants over scrubbing (Patel and Bullmore, 2015; Yang et al., 2019), and methods relying on an independent component analysis (ICA) decomposition of the data (Salimi-Khorshidi et al., 2014; Pruim et al., 2015).

Future motion correction strategies shall improve over current ones in several ways: first, through more elaborate acquisition schemes, such as with multi-echo sequences (Power et al., 2018); second, through the exploration of other complementary denoising strategies, such as with fMRI simulators (Drobnjak et al., 2006) or prospective correction (Zaitsev et al., 2017); third, and perhaps most importantly, through an efficient cross-talk across these strategies. For example, it was recently shown that the use of customised head molds reduces motion during scanning on young subjects (Power et al., 2019b); this could be pushed further by orienting the design in subject-specific manner, using motion characteristics such as the ones described here.

5. Conclusion

We demonstrated that head motion in the MR scanner during RS fMRI acquisitions, an infamous confounding factor of this imaging modality, exhibits spatio-temporal structure that is not fully accounted for by motion correction strategies. Strikingly, one’s motion characteristics can inform not only about one’s anthropometry, but, more surprisingly, about one’s behaviour and psychiatric functions. We hope that our findings will lead future clinical or cognitive fMRI studies to probe more extensively for the presence of motion-related artefacts.

Authors’ contributions

Thomas Bolton performed all the analyses, and wrote the manuscript. Valeria Kebets provided the behavioural data of the validation dataset. Enrico Glerean provided the motion time courses of the validation dataset. Daniela Zöller provided a Partial Least Squares MATLAB implementation from which part of the performed analyses were developed. Jingwei Li and Thomas Yeo provided the behavioural data of the main dataset. César Caballero-Gaudes and Dimitri Van De Ville provided extensive suggestions of improvement regarding the analyses and the manuscript content. All authors reread the manuscript.

Appendix A. Supplementary data

Supplementary data to this article can be found online at https://doi.org/10.1016/j.neuroimage.2019.116433.

References

Achenbach, T.M., 2009. The Achenbach System of Empirically Based Assessment (ASEBA): Development, Findings, Theory, and Applications. University of Vermont, Research Center for Children, Youth & Families.

Barch, D.M., Burgess, G.C., Harms, M.P., Petersen, S.E., Schlaggar, B.L., Corbetta, M., Glasser, M.F., Curtiss, S., Dixit, S., Feldt, C., et al., 2013. Function in the human connectome: task-fMRI and individual differences in behavior. Neuroimage 80, 169–189.

Bianciardi, M., Fukunaga, M., van Gelderen, P., Horovitz, S., de Zwart, J., Shmueli, K., Duyn, J., 2009. Sources of functional magnetic resonance imaging signal fluctuations in the human brain at rest: a 7 T study. Magn. Reson. Imag. 27, 1019–1029. https://doi.org/10.1016/j.mri.2009.02.004 pmid:19375260.

Birn, R.M., 2012. The role of physiological noise in resting-state functional connectivity. Neuroimage 62, 864–870. https://doi.org/10.1016/j.neuroimage.2012.01.016 pmid:22245341.

Biswal, B., Zerrin Yetkin, F., Haughton, V.M., Hyde, J.S., 1995. Functional connectivity in the motor cortex of resting human brain using echo-planar mri. Magn. Reson. Med. 34, 537–541.

Bright, M.G., Murphy, K., 2015. Is fMRI "noise" really noise? Resting state nuisance regressors remove variance with network structure. Neuroimage 114, 158–169. https://doi.org/10.1016/j.neuroimage.2015.03.070 pmid:25862264.

Burgess, G.C., Kandala, S., Nolan, D., Laumann, T.O., Power, J.D., Adeyemo, B., Barch, D.M., 2016. Evaluation of denoising strategies to address motion-correlated artifacts in resting-state functional magnetic resonance imaging data from the human connectome project. Brain Connect. 6, 669–680. https://doi.org/10.1089/brain.2016.0435 pmid:27571276.

Buysse, D.J., et al., 1989. The Pittsburgh Sleep Quality Index: a new instrument for psychiatric practice and research. Psychiatry Res. 28, 193–213. https://doi.org/10.1016/0165-1781(89)90047-4 pmid:2748771.

Caballero-Gaudes, C., Reynolds, R.C., 2017. Methods for cleaning the BOLD fMRI signal. Neuroimage 154, 128–149. https://doi.org/10.1016/j.neuroimage.2016.12.018. https://ac.els-cdn.com/S1053811916307418/1-s2.0-S1053811916307418-main.pdf?{_}tid=4d9da1b6-0cf3-11e8-b44b-00000aab0f26{&}acdnat=1518110155{_}67628ffd221945d1474611a55f364f34.

Chen, J., Liu, J., Calhoun, V.D., 2019. Translational potential of neuroimaging genomic analyses to diagnosis and treatment in mental disorders. Proc. IEEE 107, 912–927.

Ciric, R., Rosen, A.F., Erus, G., Cieslak, M., Adebimpe, A., Cook, P.A., Satterthwaite, T., 2018. Mitigating head motion artifact in functional connectivity MRI. Nat. Protoc. 13, 2801. https://doi.org/10.1038/s41596-018-0065-y pmid:30446748.

Ciric, R., Wolf, D.H., Power, J.D., Roalf, D.R., Baum, G.L., Ruparel, K., Shinohara, R.T., Elliott, M.A., Eickhoff, S.B., Davatzikos, C., Gur, R.C., Gur, R.E., Bassett, D.S., Satterthwaite, T.D., 2017. Benchmarking of participant-level confound regression strategies for the control of motion artifact in studies of functional connectivity. Neuroimage 154, 174–187. https://doi.org/10.1016/j.neuroimage.2017.03.020 arXiv:1608.03616. https://ac.els-cdn.com/S1053811917302288/1-s2.0-S1053811917302288-main.pdf?{_}tid=4031e1d6-10bd-11e8-a578-00000aab0f02{&}acdnat=1518526745{_}cc06c9eb781f7de222d112ec786e613d.

Couvy-Duchesne, B., Blokland, G.A.M., Hickie, I.B., Thompson, P.M., Martin, N.G., de Zubicaray, G.I., McMahon, K.L., Wright, M.J., 2014. Heritability of head motion during resting state functional mri in 462 healthy twins. Neuroimage 102, 424–434.

Couvy-Duchesne, B., Ebejer, J.L., Gillespie, N.A., Duffy, D.L., Hickie, I.B., Thompson, P.M., Martin, N.G., de Zubicaray, G.I., McMahon, K.L., Medland, S.E., et al., 2016. Head motion and inattention/hyperactivity share common genetic influences: implications for fmri studies of adhd. PLoS One 11, 0146271.

Damoiseaux, J.S., Rombouts, S.A.R., Barkhof, F., Scheltens, P., Stam, C.J., Smith, S.M., Beckmann, C.F., 2006. Consistent resting-state networks across healthy subjects. Proc. Natl. Acad. Sci. 103, 13848–13853. https://doi.org/10.1073/pnas.0601417103. http://www.pnas.org/content/103/37/13848.short.

Deen, B., Pelphrey, K., 2012. Perspective: brain scans need a rethink. Nature 491, 20. https://doi.org/10.1038/491S20a pmid:23136657.

Drobnjak, I., Gavaghan, D., Süli, E., Pitt-Francis, J., Jenkinson, M., 2006. Development of a functional magnetic resonance imaging simulator for modeling realistic rigid-body motion artifacts. Magn. Reson. Med. 56, 364–380.

Ekhtiari, H., Kuplicki, R., Yeh, H., Paulus, M.P., 2019. Physical characteristics not psychological state or trait characteristics predict motion during resting state fmri. Sci. Rep. 9, 419.

Engelhardt, L.E., Roe, M.A., Juranek, J., DeMaster, D., Harden, K.P., Tucker-Drob, E.M., Church, J.A., 2017. Children's head motion during fmri tasks is heritable and stable over time. Dev. Cogn. Neurosci. 25, 58–68.

Finn, E.S., et al., 2015. Functional connectome fingerprinting: identifying individuals using patterns of brain connectivity. Nat. Neurosci. 18, 1664. https://doi.org/10.1038/nn.4135 pmid:26457551.

Folstein, M.F., Lee, N.R., Helzer, J.E., 1983. The mini-mental state examination, 812–812 Arch. Gen. Psychiatr. 40. https://doi.org/10.1001/archpsyc.1983.01790060110016. pmid:6860082.

Fox, M.D., Greicius, M., 2010. Clinical applications of resting state functional connectivity. Front. Syst. Neurosci. 4, 19. https://doi.org/10.3389/fnsys.2010.00019 pmid:20592951.

Friston, K.J., Williams, S., Howard, R., Frackowiak, R.S.J., Turner, R., 1996. Movement-related effects in fMRI time-series. Magn. Reson. Med. 35, 346–355. https://doi.org/10.1002/mrm.1910350312.

Garrett, D.D., Kovacevic, N., McIntosh, A.R., Grady, C.L., 2010. Blood oxygen level-dependent signal variability is more than just noise. J. Neurosci. 30, 4914–4921.

Gershon, R.C., et al., 2010. Assessment of neurological and behavioural function: the NIH toolbox. Lancet Neurol. 9, 138–139. https://doi.org/10.1016/S1474-4422(09)70335-7 pmid:20129161.

Gu, Q., Li, Z., Han, J., 2012. Generalized Fisher Score for Feature Selection. ArXiv (DOI: 1202.3725).

Hodgson, K., Poldrack, R.A., Curran, J.E., Knowles, E.E., Mathias, S., Göring, H.H.H., Yao, N., Olvera, R.L., Fox, P.T., Almasy, L., et al., 2016. Shared genetic factors influence head motion during mri and body mass index. Cerebr. Cortex 27, 5539–5546.

Hsu, W.T., Rosenberg, M.D., Scheinost, D., Constable, R.T., Chun, M.M., 2018. Resting-state functional connectivity predicts neuroticism and extraversion in novel individuals. Soc. Cogn. Affect. Neurosci. 13, 224–232. https://doi.org/10.1093/scan/nsy002 pmid:29373729.

Jenkinson, M., Bannister, P., Brady, M., Smith, S.M., 2002. Improved optimization for the robust and accurate linear registration and motion correction of brain images. Neuroimage 17, 825–841.

Jenkinson, M., Beckmann, C.F., Behrens, T.E.J., Woolrich, M.W., Smith, S.M., 2012. FSL. Neuroimage 62, 782–790.

Kebets, V., Holmes, A.J., Orban, C., Tang, S., Li, J., Sun, N., Kong, R., P, R.A., Yeo, B.T.T., 2019. Somatosensory-motor dysconnectivity spans multiple transdiagnostic dimensions of psychopathology. Biol. Psychiatry 86, 779–791.

Kong, X., Zhen, Z., Li, X., Lu, H., Wang, R., Liu, L., He, Y., Zang, Y., Liu, J., 2014. Individual differences in impulsivity predict head motion during magnetic resonance imaging. PLoS One 9, 104989.

Krishnan, A., Williams, L.J., McIntosh, A.R., Abdi, H., 2011. Partial least squares (PLS) methods for neuroimaging: a tutorial and review. Neuroimage 56, 455–475. https://doi.org/10.1016/j.neuroimage.2010.07.034. http://www.sciencedirect.com/science/article/pii/S1053811910010074.

Kuhn, H.W., 1955. The Hungarian method for the assignment problem. Nav. Res. Logist. Q. 2, 83–97.

Laumann, T.O., Snyder, A.Z., Mitra, A., Gordon, E.M., Gratton, C., Adeyemo, B., Gilmore, A.W., Nelson, S.M., Berg, J.J., Greene, D.J., et al., 2016. On the stability of bold fmri correlations. Cerebr. Cortex 27, 4719–4732.

Lemieux, L., Salek-Haddadi, A., Lund, T.E., Laufs, H., Carmichael, D., 2007. Modelling large motion events in fMRI studies of patients with epilepsy. Magn. Reson. Imag. 25, 894–901. https://doi.org/10.1016/j.mri.2007.03.009. https://ac.els-cdn.com/S0730725X07002214/1-s2.0-S0730725X07002214-main.pdf?{_}tid=92ab5ebe-10e1-11e8-896b-00000aab0f6b{&}acdnat=1518542345{_}95c2427b8c8503be33bf2746e05ba024.

Liu, T.T., 2016. Noise contributions to the fMRI signal: an overview. Neuroimage 143, 141–151. https://doi.org/10.1016/j.neuroimage.2016.09.008 pmid:27612646.

Makowski, C., Lepage, M., Evans, A., 2019. Head motion: the dirty little secret of neuroimaging in psychiatry. J. Psychiatry Neurosci. 44, 62. https://doi.org/10.1503/jpn.180022 pmid:30565907.

McCrae, R.R., Costa Jr., P.T., 2004. A contemplated revision of the neo five-factor inventory. Personal. Individ. Differ. 36, 587–596.

McIntosh, A.R., Lobaugh, N.J., 2004. Partial least squares analysis of neuroimaging data: applications and advances. Neuroimage 23, 250–263. https://doi.org/10.1016/j.neuroimage.2004.07.020. http://www.sciencedirect.com/science/article/pii/S1053811904003866.

Parkes, L., Fulcher, B., Yücel, M., Fornito, A., 2018. An evaluation of the efficacy, reliability, and sensitivity of motion correction strategies for resting-state functional MRI. Neuroimage 171, 415–436. https://doi.org/10.1016/j.neuroimage.2017.12.073 pmid:29278773.

Patel, A.X., Bullmore, E.T., 2015. A wavelet-based estimator of the degrees of freedom in denoised fmri time series for probabilistic testing of functional connectivity and brain graphs. Neuroimage 142, 14–26.

Patriat, R., Molloy, E.K., Birn, R.M., 2015. Using edge voxel information to improve motion regression for rs-fMRI connectivity studies. Brain Connect. 5, 582–595. https://doi.org/10.1089/brain.2014.0321 pmid:26107049.

Patriat, R., Reynolds, R.C., Birn, R.M., 2017. An improved model of motion-related signal changes in fMRI. Neuroimage 144, 74–82. https://doi.org/10.1016/j.neuroimage.2016.08.051 pmid:27570108.

Poldrack, R.A., Congdon, E., Triplett, W., Gorgolewski, K.J., Karlsgodt, K.H., Mumford, J.A., Sabb, F.W., Freimer, N.B., London, E.D., Cannon, T.D., et al., 2016. A phenome-wide examination of neural and cognitive function. Sci. Data 3, 160110.

Power, J.D., Barnes, K.A., Snyder, A.Z., Schlaggar, B.L., Petersen, S.E., 2012. Spurious but systematic correlations in functional connectivity MRI networks arise from subject motion. Neuroimage 59, 2142–2154.

Power, J.D., Cohen, A.L., Nelson, S.M., Wig, G.S., Barnes, K.A., Church, J.A., Vogel, A.C., Laumann, T.O., Miezin, F.M., Schlaggar, B.L., et al., 2011. Functional network organization of the human brain. Neuron 72, 665–678.

Power, J.D., Mitra, A., Laumann, T.O., Snyder, A.Z., Schlaggar, B.L., Petersen, S.E., 2014. Methods to detect, characterize, and remove motion artifact in resting state fMRI. Neuroimage 84, 320–341. https://doi.org/10.1016/j.neuroimage.2013.08.048 arXiv:NIHMS150003. http://linkinghub.elsevier.com/retrieve/pii/S1053811913009117.

Power, J.D., Plitt, M., Gotts, S.J., Kundu, P., Voon, V., Bandettini, P.A., Martin, A., 2018. Ridding fMRI data of motion-related influences: removal of signals with distinct spatial and physical bases in multiecho data. Proc. Natl. Acad. Sci. 115, 2105–2114. https://doi.org/10.1073/pnas.1720985115 pmid:29440410.

Power, J.D., Schlaggar, B.L., Petersen, S.E., 2015. Recent progress and outstanding issues in motion correction in resting state fmri. Neuroimage 105, 536–551.

Power, J.D., Silver, B.M., Dubin, M.J., Martin, A., Jones, R.M., 2019a. Distinctions Among Real and Apparent Respiratory Motions in Human fMRI Data.

Power, J.D., Silver, B.M., Silverman, M.R., Ajodan, E.L., Bos, D.J., Jones, R.M., 2019b. Customized head molds reduce motion during resting state fmri scans. Neuroimage 189, 141–149.

Preti, M.G., Bolton, T.A.W., Van De Ville, D., 2017. The dynamic functional connectome: state-of-the-art and perspectives. Neuroimage 160, 41–54. https://doi.org/10.1016/j.neuroimage.2016.12.061 arXiv:1511.02976. https://ac.els-cdn.com/S1053811916307881/1-s2.0-S1053811916307881-main.pdf?{_}tid=740fef8f-835b-4993-86d3-a6f60b841679{&}acdnat=1523360042{_}29ea611d8892cbd9e44c8ac92ff16e62.

Pruim, R.H., Mennes, M., van Rooij, D., Llera, A., Buitelaar, J.K., Beckmann, C.F., 2015. ICA-AROMA: a robust ICA-based strategy for removing motion artifacts from fMRI data. Neuroimage 112, 267–277. https://doi.org/10.1016/j.neuroimage.2015.02.064 pmid:25770991.

Rosenberg, M.D., Finn, E.S., Scheinost, D., Papademetris, X., Shen, X., Constable, R.T., Chun, M.M., 2016. A neuromarker of sustained attention from whole-brain functional connectivity. Nat. Neurosci. 19, 165. https://doi.org/10.1038/nn.4179 pmid:26595653.

Salimi-Khorshidi, G., Douaud, G., Beckmann, C., Glasser, M., Griffanti, L., Smith, S., 2014. Automatic denoising of functional MRI data: combining independent component analysis and hierarchical fusion of classifiers. Neuroimage 90, 449–468. https://doi.org/10.1016/j.neuroimage.2013.11.046 pmid:24389422.

Satterthwaite, T.D., Elliott, M.A., Gerraty, R.T., Ruparel, K., Loughead, J., Calkins, M.E., Eickhoff, S.B., Hakonarson, H., Gur, R.C., Gur, R.E., Wolf, D.H., 2013. An improved framework for confound regression and filtering for control of motion artifact in the preprocessing of resting-state functional connectivity data. Neuroimage 64, 240–256. https://doi.org/10.1016/j.neuroimage.2012.08.052 arXiv:NIHMS150003. https://ac.els-cdn.com/S1053811912008609/1-s2.0-S105381191200860 9-main.pdf?{_}tid=6eb8e364-10b9-11e8-a7ff-00000aab0f6b{&}acdnat=151852510 5{_}f7e9a92d77f9084f6b5d4fee9fd3afcf.

Satterthwaite, T.D., Wolf, D.H., Loughead, J., Ruparel, K., Elliott, M.A., Hakonarson, H., Gur, R.C., Gur, R.E., 2012. Impact of in-scanner head motion on multiple measures of functional connectivity : relevance for studies of neurodevelopment in youth. Neuroimage 60, 623–632. https://doi.org/10.1016/j.neuroimage.2011.12.063. http://ac.els-cdn.com/S1053811911014650/1-s2.0-S1053811911014650-main.pdf ?{_}tid=edf9d138-e3ce-11e6-bb29-00000aab0f6c{&}acdnat=1485439037{_}633f 9a9e6b0b068775f861fadf339f66.

Siegel, J.S., Mitra, A., Laumann, T.O., Seitzman, B.A., Raichle, M., Corbetta, M., Snyder, A.Z., 2016. Data quality influences observed links between functional connectivity and behavior. Cerebr. Cortex 27, 4492–4502.

Smith, S.M., Beckmann, C.F., Andersson, J., Auerbach, E.J., Bijsterbosch, J., Douaud, G., Duff, E., Feinberg, D.A., Griffanti, L., Harms, M.P., et al., 2013. Resting-state fmri in the human connectome project. Neuroimage 80, 144–168.

Smith, S.M., Nichols, T.E., Vidaurre, D., Winkler, A.M., Behrens, T.E.J., Glasser, M.F., Ugurbil, K., Barch, D.M., Van Essen, D.C., Miller, K.L., 2015. A positive-negative mode of population covariation links brain connectivity, demographics and behavior. Nat. Neurosci. 18, 1565–1567. https://doi.org/10.1038/nn.4125. http://www.n ature.com/doifinder/10.1038/nn.4125.

Van Dijk, K.R., Hedden, T., Venkataraman, A., Evans, K.C., Lazar, S.W., Buckner, R.L., 2009. Intrinsic functional connectivity as a tool for human connectomics: theory, properties, and optimization. J. Neurophysiol. 103, 297–321. https://doi.org/ 10.1152/jn.00783.2009 pmid:19889849.

Van Dijk, K.R., Sabuncu, M.R., Buckner, R.L., 2012. The influence of head motion on intrinsic functional connectivity MRI. Neuroimage 59, 431–438. https://doi.org/ 10.1016/j.neuroimage.2011.07.044 pmid:21810475.

Von Luxburg, U., 2007. A tutorial on spectral clustering. Stat. Comput. 17, 395–416.

Watanabe, T., Sasaki, Y., Shibata, K., Kawato, M., 2017. Advances in fMRI real-time neurofeedback. Trends Cogn. Sci. 21, 997–1010. https://doi.org/10.1016/ j.tics.2017.09.010 pmid:29031663.

Wilke, M., 2014. Isolated assessment of translation or rotation severely underestimates the effects of subject motion in fMRI data. PLoS One 9, 106498. https://doi.org/ 10.1371/journal.pone.0106498 pmid:25333359.

Wylie, G.R., Genova, H., DeLuca, J., Chiaravalloti, N., Sumowski, J.F., 2014. Functional magnetic resonance imaging movers and shakers: does subject-movement cause sampling bias? Hum. Brain Mapp. 35, 1–13.

Yan, C., Cheung, B., Kelly, C., Colcombe, S., Craddock, R.C., Di Martino, A., Li, Q., Zuo, X., Castellanos, F.X., Milham, M.P., 2013. A comprehensive assessment of regional variation in the impact of head micromovements on functional connectomics. Neuroimage 76, 183–201.

Yang, Z., Zhuang, X., Screenivasan, K., Mishra, V., Cordes, D., 2019. Robust motion regression of resting-state data using a convolutional neural network model. Front. Neurosci. 13, 169. https://doi.org/10.3389/fnins.2019.00169 pmid:31057348.

Yeo, B.T.T., Krienen, F.M., Sepulcre, J., Sabuncu, M.R., Lashkari, D., Hollinshead, M., Roffman, J.L., Smoller, J.W., Zöllei, L., Polimeni, J.R., et al., 2011. The organization of the human cerebral cortex estimated by intrinsic functional connectivity. J. Neurophysiol. 106, 1125–1165.

Zaitsev, M., Akin, B., LeVan, P., Knowles, B.R., 2017. Prospective motion correction in functional mri. Neuroimage 154, 33–42.

Zeng, L., Wang, D., Fox, M.D., Sabuncu, M., Hu, D., Ge, M., Buckner, R.L., Liu, H., 2014. Neurobiological basis of head motion in brain imaging. Proc. Natl. Acad. Sci. 111, 6058–6062.

Zöller, D., Schaer, M., Scariati, E., Padula, M., Eliez, S., Van De Ville, D., 2017. Disentangling resting-state BOLD variability and PCC functional connectivity in 22q11. 2 deletion syndrome. Neuroimage 149, 85–97. https://doi.org/10.1016/ j.neuroimage.2017.01.064 pmid:28143774.